FERMILAB-PUB-09-299-E

Search for Higgs boson decay to neutral long-lived particles decaying to $b\bar{b}$ in $p\bar{p}$ collisions at $\sqrt{s} = 1.96$ TeV

V.M. Abazov[37], B. Abbott[75], M. Abolins[65], B.S. Acharya[30], M. Adams[51], T. Adams[49], E. Aguilo[6], M. Ahsan[59], G.D. Alexeev[37], G. Alkhazov[41], A. Alton[64,a], G. Alverson[63], G.A. Alves[2], L.S. Ancu[36], T. Andeen[53], M.S. Anzelc[53], M. Aoki[50], Y. Arnoud[14], M. Arov[60], M. Arthaud[18], A. Askew[49,b], B. Åsman[42], O. Atramentov[49,b], C. Avila[8], J. BackusMayes[82], F. Badaud[13], L. Bagby[50], B. Baldin[50], D.V. Bandurin[59], S. Banerjee[30], E. Barberis[63], A.-F. Barfuss[15], P. Bargassa[80], P. Baringer[58], J. Barreto[2], J.F. Bartlett[50], U. Bassler[18], D. Bauer[44], S. Beale[6], A. Bean[58], M. Begalli[3], M. Begel[73], C. Belanger-Champagne[42], L. Bellantoni[50], A. Bellavance[50], J.A. Benitez[65], S.B. Beri[28], G. Bernardi[17], R. Bernhard[23], I. Bertram[43], M. Besançon[18], R. Beuselinck[44], V.A. Bezzubov[40], P.C. Bhat[50], V. Bhatnagar[28], G. Blazey[52], S. Blessing[49], K. Bloom[67], A. Boehnlein[50], D. Boline[62], T.A. Bolton[59], E.E. Boos[39], G. Borissov[43], T. Bose[62], A. Brandt[78], R. Brock[65], G. Brooijmans[70], A. Bross[50], D. Brown[19], X.B. Bu[7], D. Buchholz[53], M. Buehler[81], V. Buescher[22], V. Bunichev[39], S. Burdin[43,c], T.H. Burnett[82], C.P. Buszello[44], P. Calfayan[26], B. Calpas[15], S. Calvet[16], J. Cammin[71], M.A. Carrasco-Lizarraga[34], E. Carrera[49], W. Carvalho[3], B.C.K. Casey[50], H. Castilla-Valdez[34], S. Chakrabarti[72], D. Chakraborty[52], K.M. Chan[55], A. Chandra[48], E. Cheu[46], D.K. Cho[62], S. Choi[33], B. Choudhary[29], T. Christoudias[44], S. Cihangir[50], D. Claes[67], J. Clutter[58], M. Cooke[50], W.E. Cooper[50], M. Corcoran[80], F. Couderc[18], M.-C. Cousinou[15], S. Crépé-Renaudin[14], D. Cutts[77], M. Ćwiok[31], A. Das[46], G. Davies[44], K. De[78], S.J. de Jong[36], E. De La Cruz-Burelo[34], K. DeVaughan[67], F. Déliot[18], M. Demarteau[50], R. Demina[71], D. Denisov[50], S.P. Denisov[40], S. Desai[50], H.T. Diehl[50], M. Diesburg[50], A. Dominguez[67], T. Dorland[82], A. Dubey[29], L.V. Dudko[39], L. Duflot[16], D. Duggan[49], A. Duperrin[15], S. Dutt[28], A. Dyshkant[52], M. Eads[67], D. Edmunds[65], J. Ellison[48], V.D. Elvira[50], Y. Enari[77], S. Eno[61], M. Escalier[15], H. Evans[54], A. Evdokimov[73], V.N. Evdokimov[40], G. Facini[63], A.V. Ferapontov[59], T. Ferbel[61,71], F. Fiedler[25], F. Filthaut[36], W. Fisher[50], H.E. Fisk[50], M. Fortner[52], H. Fox[43], S. Fu[50], S. Fuess[50], T. Gadfort[70], C.F. Galea[36], A. Garcia-Bellido[71], V. Gavrilov[38], P. Gay[13], W. Geist[19], W. Geng[15,65], C.E. Gerber[51], Y. Gershtein[49,b], D. Gillberg[6], G. Ginther[50,71], B. Gómez[8], A. Goussiou[82], P.D. Grannis[72], S. Greder[19], H. Greenlee[50], Z.D. Greenwood[60], E.M. Gregores[4], G. Grenier[20], Ph. Gris[13], J.-F. Grivaz[16], A. Grohsjean[18], S. Grünendahl[50], M.W. Grünewald[31], F. Guo[72], J. Guo[72], G. Gutierrez[50], P. Gutierrez[75], A. Haas[70], P. Haefner[26], S. Hagopian[49], J. Haley[68], I. Hall[65], R.E. Hall[47], L. Han[7], K. Harder[45], A. Harel[71], J.M. Hauptman[57], J. Hays[44], T. Hebbeker[21], D. Hedin[52], J.G. Hegeman[35], A.P. Heinson[48], U. Heintz[62], C. Hensel[24], I. Heredia-De La Cruz[34], K. Herner[64], G. Hesketh[63], M.D. Hildreth[55], R. Hirosky[81], T. Hoang[49], J.D. Hobbs[72], B. Hoeneisen[12], M. Hohlfeld[22], S. Hossain[75], P. Houben[35], Y. Hu[72], Z. Hubacek[10], N. Huske[17], V. Hynek[10], I. Iashvili[69], R. Illingworth[50], A.S. Ito[50], S. Jabeen[62], M. Jaffré[16], S. Jain[75], K. Jakobs[23], D. Jamin[15], R. Jesik[44], K. Johns[46], C. Johnson[70], M. Johnson[50], D. Johnston[67], A. Jonckheere[50], P. Jonsson[44], A. Juste[50], E. Kajfasz[15], D. Karmanov[39], P.A. Kasper[50], I. Katsanos[67], V. Kaushik[78], R. Kehoe[79], S. Kermiche[15], N. Khalatyan[50], A. Khanov[76], A. Kharchilava[69], Y.N. Kharzheev[37], D. Khatidze[70], T.J. Kim[32], M.H. Kirby[53], M. Kirsch[21], B. Klima[50], J.M. Kohli[28], J.-P. Konrath[23], A.V. Kozelov[40], J. Kraus[65], T. Kuhl[25], A. Kumar[69], A. Kupco[11], T. Kurča[20], V.A. Kuzmin[39], J. Kvita[9], F. Lacroix[13], D. Lam[55], S. Lammers[54], G. Landsberg[77], P. Lebrun[20], W.M. Lee[50], A. Leflat[39], J. Lellouch[17], J. Li[78,‡], L. Li[48], Q.Z. Li[50], S.M. Lietti[5], J.K. Lim[32], D. Lincoln[50], J. Linnemann[65], V.V. Lipaev[40], R. Lipton[50], Y. Liu[7], Z. Liu[6], A. Lobodenko[41], M. Lokajicek[11], P. Love[43], H.J. Lubatti[82], R. Luna-Garcia[34,d], A.L. Lyon[50], A.K.A. Maciel[2], D. Mackin[80], P. Mättig[27], R. Magaña-Villalba[34], A. Magerkurth[64], P.K. Mal[46], H.B. Malbouisson[3], S. Malik[67], V.L. Malyshev[37], Y. Maravin[59], B. Martin[14], R. McCarthy[72], C.L. McGivern[58], M.M. Meijer[36], A. Melnitchouk[66], L. Mendoza[8], D. Menezes[52], P.G. Mercadante[5], M. Merkin[39], K.W. Merritt[50], A. Meyer[21], J. Meyer[24], J. Mitrevski[70], N.K. Mondal[30], R.W. Moore[6], T. Moulik[58], G.S. Muanza[15], M. Mulhearn[70], O. Mundal[22], L. Mundim[3], E. Nagy[15], M. Naimuddin[50], M. Narain[77], H.A. Neal[64], J.P. Negret[8], P. Neustroev[41], H. Nilsen[23], H. Nogima[3], S.F. Novaes[5], T. Nunnemann[26], G. Obrant[41], C. Ochando[16], D. Onoprienko[59], J. Orduna[34], N. Oshima[50], N. Osman[44], J. Osta[55], R. Otec[10], G.J. Otero y Garzón[1], M. Owen[45], M. Padilla[48], P. Padley[80], M. Pangilinan[77], N. Parashar[56], S.-J. Park[24], S.K. Park[32], J. Parsons[70], R. Partridge[77], N. Parua[54], A. Patwa[73], G. Pawloski[80], B. Penning[23], M. Perfilov[39], K. Peters[45], Y. Peters[45], P. Pétroff[16], R. Piegaia[1], J. Piper[65], M.-A. Pleier[22], P.L.M. Podesta-Lerma[34,e], V.M. Podstavkov[50], Y. Pogorelov[55], M.-E. Pol[2], P. Polozov[38], A.V. Popov[40], W.L. Prado da Silva[3], S. Protopopescu[73], J. Qian[64], A. Quadt[24], B. Quinn[66], A. Rakitine[43], M.S. Rangel[16], K. Ranjan[29], P.N. Ratoff[43], P. Renkel[79], P. Rich[45], M. Rijssenbeek[72], I. Ripp-Baudot[19], F. Rizatdinova[76], S. Robinson[44], M. Rominsky[75], C. Royon[18], P. Rubinov[50], R. Ruchti[55], G. Safronov[38], G. Sajot[14], A. Sánchez-Hernández[34], M.P. Sanders[26], B. Sanghi[50], G. Savage[50], L. Sawyer[60], T. Scanlon[44], D. Schaile[26], R.D. Schamberger[72], Y. Scheglov[41], H. Schellman[53], T. Schliephake[27], S. Schlobohm[82], C. Schwanenberger[45], R. Schwienhorst[65], J. Sekaric[49], H. Severini[75], E. Shabalina[24], M. Shamim[59], V. Shary[18], A.A. Shchukin[40], R.K. Shivpuri[29], V. Siccardi[19], V. Simak[10], V. Sirotenko[50], P. Skubic[75], P. Slattery[71], D. Smirnov[55], G.R. Snow[67], J. Snow[74], S. Snyder[73], S. Söldner-Rembold[45], L. Sonnenschein[21], A. Sopczak[43], M. Sosebee[78], K. Soustruznik[9], B. Spurlock[78], J. Stark[14], V. Stolin[38], D.A. Stoyanova[40], J. Strandberg[64], M.A. Strang[69], E. Strauss[72], M. Strauss[75], R. Ströhmer[26], D. Strom[53], L. Stutte[50], S. Sumowidagdo[49], P. Svoisky[36], M. Takahashi[45], A. Tanasijczuk[1], W. Taylor[6], B. Tiller[26], M. Titov[18], V.V. Tokmenin[37], I. Torchiani[23], D. Tsybychev[72], B. Tuchming[18], C. Tully[68], P.M. Tuts[70], R. Unalan[65], L. Uvarov[41], S. Uvarov[41], S. Uzunyan[52], P.J. van den Berg[35], R. Van Kooten[54], W.M. van Leeuwen[35], N. Varelas[51], E.W. Varnes[46], I.A. Vasilyev[40], P. Verdier[20], L.S. Vertogradov[37], M. Verzocchi[50], D. Vilanova[18], P. Vint[44], P. Vokac[10], M. Voutilainen[67,f], R. Wagner[68], H.D. Wahl[49], M.H.L.S. Wang[71], J. Warchol[55], G. Watts[82], M. Wayne[55], G. Weber[25], M. Weber[50,g], L. Welty-Rieger[54], A. Wenger[23,h], M. Wetstein[61], A. White[78], D. Wicke[25], M.R.J. Williams[43], G.W. Wilson[58], S.J. Wimpenny[48], M. Wobisch[60], D.R. Wood[63], T.R. Wyatt[45], Y. Xie[77], C. Xu[64], S. Yacoob[53], R. Yamada[50], W.-C. Yang[45], T. Yasuda[50], Y.A. Yatsunenko[37], Z. Ye[50], H. Yin[7], K. Yip[73], H.D. Yoo[77], S.W. Youn[53], J. Yu[78], C. Zeitnitz[27], S. Zelitch[81], T. Zhao[82], B. Zhou[64], J. Zhu[72], M. Zielinski[71], D. Zieminska[54], L. Zivkovic[70], V. Zutshi[52], and E.G. Zverev[39]

(The DØ Collaboration)

[1] *Universidad de Buenos Aires, Buenos Aires, Argentina*
[2] *LAFEX, Centro Brasileiro de Pesquisas Físicas, Rio de Janeiro, Brazil*
[3] *Universidade do Estado do Rio de Janeiro, Rio de Janeiro, Brazil*
[4] *Universidade Federal do ABC, Santo André, Brazil*
[5] *Instituto de Física Teórica, Universidade Estadual Paulista, São Paulo, Brazil*
[6] *University of Alberta, Edmonton, Alberta, Canada; Simon Fraser University, Burnaby, British Columbia, Canada; York University, Toronto, Ontario, Canada and McGill University, Montreal, Quebec, Canada*
[7] *University of Science and Technology of China, Hefei, People's Republic of China*
[8] *Universidad de los Andes, Bogotá, Colombia*
[9] *Center for Particle Physics, Charles University, Faculty of Mathematics and Physics, Prague, Czech Republic*
[10] *Czech Technical University in Prague, Prague, Czech Republic*
[11] *Center for Particle Physics, Institute of Physics, Academy of Sciences of the Czech Republic, Prague, Czech Republic*
[12] *Universidad San Francisco de Quito, Quito, Ecuador*
[13] *LPC, Université Blaise Pascal, CNRS/IN2P3, Clermont, France*
[14] *LPSC, Université Joseph Fourier Grenoble 1, CNRS/IN2P3, Institut National Polytechnique de Grenoble, Grenoble, France*
[15] *CPPM, Aix-Marseille Université, CNRS/IN2P3, Marseille, France*
[16] *LAL, Université Paris-Sud, IN2P3/CNRS, Orsay, France*
[17] *LPNHE, IN2P3/CNRS, Universités Paris VI and VII, Paris, France*
[18] *CEA, Irfu, SPP, Saclay, France*
[19] *IPHC, Université de Strasbourg, CNRS/IN2P3, Strasbourg, France*
[20] *IPNL, Université Lyon 1, CNRS/IN2P3, Villeurbanne, France and Université de Lyon, Lyon, France*
[21] *III. Physikalisches Institut A, RWTH Aachen University, Aachen, Germany*
[22] *Physikalisches Institut, Universität Bonn, Bonn, Germany*
[23] *Physikalisches Institut, Universität Freiburg, Freiburg, Germany*
[24] *II. Physikalisches Institut, Georg-August-Universität Göttingen, Göttingen, Germany*
[25] *Institut für Physik, Universität Mainz, Mainz, Germany*
[26] *Ludwig-Maximilians-Universität München, München, Germany*
[27] *Fachbereich Physik, University of Wuppertal, Wuppertal, Germany*
[28] *Panjab University, Chandigarh, India*
[29] *Delhi University, Delhi, India*
[30] *Tata Institute of Fundamental Research, Mumbai, India*
[31] *University College Dublin, Dublin, Ireland*
[32] *Korea Detector Laboratory, Korea University, Seoul, Korea*
[33] *SungKyunKwan University, Suwon, Korea*
[34] *CINVESTAV, Mexico City, Mexico*

[35] FOM-Institute NIKHEF and University of Amsterdam/NIKHEF, Amsterdam, The Netherlands
[36] Radboud University Nijmegen/NIKHEF, Nijmegen, The Netherlands
[37] Joint Institute for Nuclear Research, Dubna, Russia
[38] Institute for Theoretical and Experimental Physics, Moscow, Russia
[39] Moscow State University, Moscow, Russia
[40] Institute for High Energy Physics, Protvino, Russia
[41] Petersburg Nuclear Physics Institute, St. Petersburg, Russia
[42] Stockholm University, Stockholm, Sweden, and Uppsala University, Uppsala, Sweden
[43] Lancaster University, Lancaster, United Kingdom
[44] Imperial College, London, United Kingdom
[45] University of Manchester, Manchester, United Kingdom
[46] University of Arizona, Tucson, Arizona 85721, USA
[47] California State University, Fresno, California 93740, USA
[48] University of California, Riverside, California 92521, USA
[49] Florida State University, Tallahassee, Florida 32306, USA
[50] Fermi National Accelerator Laboratory, Batavia, Illinois 60510, USA
[51] University of Illinois at Chicago, Chicago, Illinois 60607, USA
[52] Northern Illinois University, DeKalb, Illinois 60115, USA
[53] Northwestern University, Evanston, Illinois 60208, USA
[54] Indiana University, Bloomington, Indiana 47405, USA
[55] University of Notre Dame, Notre Dame, Indiana 46556, USA
[56] Purdue University Calumet, Hammond, Indiana 46323, USA
[57] Iowa State University, Ames, Iowa 50011, USA
[58] University of Kansas, Lawrence, Kansas 66045, USA
[59] Kansas State University, Manhattan, Kansas 66506, USA
[60] Louisiana Tech University, Ruston, Louisiana 71272, USA
[61] University of Maryland, College Park, Maryland 20742, USA
[62] Boston University, Boston, Massachusetts 02215, USA
[63] Northeastern University, Boston, Massachusetts 02115, USA
[64] University of Michigan, Ann Arbor, Michigan 48109, USA
[65] Michigan State University, East Lansing, Michigan 48824, USA
[66] University of Mississippi, University, Mississippi 38677, USA
[67] University of Nebraska, Lincoln, Nebraska 68588, USA
[68] Princeton University, Princeton, New Jersey 08544, USA
[69] State University of New York, Buffalo, New York 14260, USA
[70] Columbia University, New York, New York 10027, USA
[71] University of Rochester, Rochester, New York 14627, USA
[72] State University of New York, Stony Brook, New York 11794, USA
[73] Brookhaven National Laboratory, Upton, New York 11973, USA
[74] Langston University, Langston, Oklahoma 73050, USA
[75] University of Oklahoma, Norman, Oklahoma 73019, USA
[76] Oklahoma State University, Stillwater, Oklahoma 74078, USA
[77] Brown University, Providence, Rhode Island 02912, USA
[78] University of Texas, Arlington, Texas 76019, USA
[79] Southern Methodist University, Dallas, Texas 75275, USA
[80] Rice University, Houston, Texas 77005, USA
[81] University of Virginia, Charlottesville, Virginia 22901, USA and
[82] University of Washington, Seattle, Washington 98195, USA

(Dated: June 9, 2009)

We report on a first search for production of Higgs bosons decaying into neutral long-lived particles (NLLP) which each decay to a $b\bar{b}$ pair, using 3.6 fb^{-1} of data recorded with the D0 detector at the Fermilab Tevatron collider. We search for pairs of displaced vertices in the tracking detector at radii in the range 1.6–20 cm from the beam axis. No significant excess is observed above background, and upper limits are set on the production rate in a hidden-valley benchmark model for a range of Higgs boson masses and NLLP masses and lifetimes.

PACS numbers: 12.60.Fr, 14.80.Cp

A class of hidden-valley (HV) models [1] predicts a new, confining gauge group that is weakly coupled to the standard model (SM), leading to the production of HV particles (v-particles). The details of v-particle decay depend on the specific model, but the HV quarks always hadronize due to confinement producing "v-hadrons" that can be long-lived. One particular model used as a benchmark for this search is the SM Higgs boson (H)

mixing with a HV Higgs boson that gives mass to v-particles. The SM Higgs boson could then decay directly to v-hadrons through this mixing with a substantial branching fraction [2]. These v-hadrons may couple preferentially to heavy SM particles, such as b quarks, due to helicity suppression. The result is a striking experimental signature of highly displaced secondary vertices (SV) with a large number of attached tracks from the b quark decays. Direct searches at the CERN LEP collider have excluded a Higgs boson decaying to $b\bar{b}$ or $\tau\bar{\tau}$ with $M_H < 114.4$ GeV at the 95% C.L. [3]. But if the Higgs boson dominantly decays to long-lived v-particles which then decay inside the detector to $b\bar{b}$, only the most general LEP limit is relevant, $M_H > 81$ GeV, for any Higgs boson radiating off a Z boson [4]. Cosmological constraints require that one of the light v-hadrons have a lifetime $\ll 1$ second to be consistent with models of big bang nucleosynthesis [1].

In this Letter, we present the first search for pair-produced neutral long-lived particles (NLLP), each decaying to a b quark pair, using the D0 detector [5] at the Fermilab Tevatron $p\overline{p}$ collider. The b quarks are required in order to provide a high transverse momentum (p_T) muon for triggering with high efficiency. The data were collected from April 2002 to August 2008 and correspond to an integrated luminosity of 3.6 fb^{-1} at $\sqrt{s} = 1.96$ TeV. The D0 central tracking detector comprises a silicon microstrip tracker (SMT) and a central fiber tracker (CFT), both located within a 2 T superconducting solenoidal magnet. The SMT, extending from a radius of $\approx$2 cm to $\approx$10 cm, has a six-barrel longitudinal structure, each with a set of four layers arranged axially around the beam pipe, and interspersed with 16 radial disks. The CFT, extending from a radius of $\approx$20 cm to $\approx$50 cm, has eight thin coaxial barrels, each supporting two doublets of overlapping scintillating fibers. Secondary vertices are reconstructed by combining charged particle tracks found in the tracking detector, which effectively limits the analysis to NLLP decays occurring within a maximum radius of 20 cm, well within the tracker volume. We also exclude vertex radii less than 1.6 cm since the background from heavy flavor production is large in that region. Known sources of SVs other than heavy-flavor include decays in-flight of light particles, inelastic interactions of particles with nuclei of detector material, and photon conversions. Vertices may also be mimicked by pattern recognition errors.

PYTHIA [6] is used to simulate signal and background events, which are then passed through a full GEANT3-based [7] D0 detector simulation and the same reconstruction as for collider data. For signal, the SM $gg{\to}H$ process is generated, the Higgs boson is forced to decay to a pair of long-lived A bosons (a heavy, neutral scalar, representing a v-hadron), and each A boson is forced to decay to a pair of b quarks. The Higgs boson mass (M_H) is varied from 90 to 200 GeV, the v-hadron mass (m_{HV}) from 15 to 40 GeV and the average v-hadron proper decay length ($L_d = c\tau$) from 2.5 cm to 10 cm. For background, inclusive $p\overline{p}$ multijet events are generated. Approximately one hundred thousand Monte Carlo (MC) events for each signal sample and ten million events of multijet background are generated and are overlaid with data to simulate detector noise and pile-up effects from additional $p\overline{p}$ interactions.

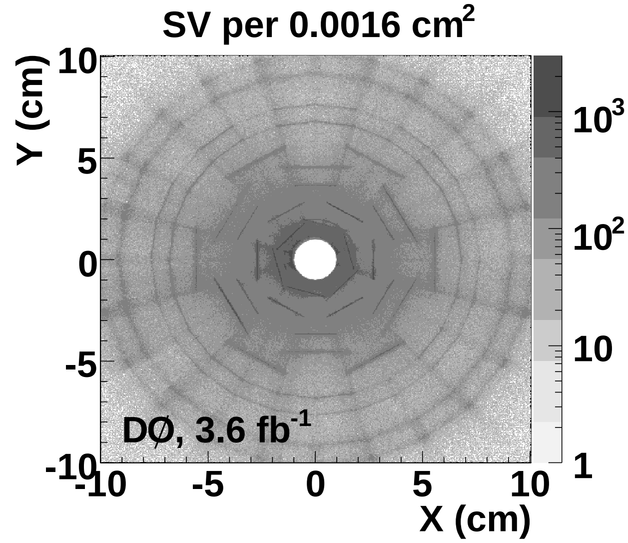

FIG. 1: Material map in the plane transverse to the beamline, generated using SVs with three attached tracks, in events passing the initial selection. The structure of the silicon detector and supports are clearly seen.

At least two jets with a cone radius of 0.5 [8] are required, each with $p_T > 10$ GeV. And at least one muon is required with $p_T > 4$ GeV, matched within $\Delta\mathcal{R} < 0.7$ to one of the jets, where $\Delta\mathcal{R} = \sqrt{(\Delta\phi)^2 + (\Delta\eta)^2}$ with ϕ being the azimuthal angle and η the pseudorapidity. The muon requirement is more efficient for signal than background due to the presence of a $b \to \mu$ or $b \to c \to \mu$ decay from at least one of the four b quarks, and is also required for an accurate measurement of the trigger efficiency. Primary vertices (PVs) are reconstructed by clustering tracks and correspond to $p\overline{p}$ interaction locations. To ensure good SV reconstruction, we further require fewer than four PVs be reconstructed and that the selected PV with the largest $\sum_i \log p_T^i$, summed over all vertex tracks i, be located within $|z| < 35$ cm and $r < 1$ cm, where x and y are the horizontal and vertical components of the distance r with respect to the beam axis, and z is the distance along the beam axis from the center of the detector. An initial selection requires that each event has at least one SV with 2D decay length from the PV in the plane transverse to the beam (L_d^{xy}) larger than 1 cm and decay length significance (decay length divided by its uncertainty) greater than five. The momentum of the SV, reconstructed from the vectorial sum of the momenta of its associated tracks, must point away from the PV to reduce combinatoric background. SVs are reconstructed using a track selection so as to efficiently combine the b and $\bar{b}$ decay products of each v-hadron into a single SV. Approximately 50 million data events satisfy these requirements, dominated by dijet and heavy-flavor production.

To maximize the discovery potential of this analysis we use an OR of all triggers. The most frequently fired triggers that make up the dataset passing the initial selection involve a muon and jet at the first trigger level and refinements of these objects at higher levels. The overall trigger OR efficiency is estimated by first measuring the efficiency for a single trigger per data collection period using known muon and jet trigger efficiencies. Then the number of events fired by that single trigger is compared to the total number of data events passing the OR of all triggers, as a function of sensitive variables, such as muon p_T, jet p_T, jet angles, etc. No significant dependence is found, except on jet p_T, thus the overall trigger OR efficiency is modeled as a function of jet p_T.

Further selections are optimized by maximizing the expected signal significance ($S/\sqrt{S+B}$), where B and S are the number of MC background and signal events, respectively. The heavy-flavor background, mainly b hadrons with $c\tau{\approx}0.3$ cm, produces a very large number of SVs, but their number decreases exponentially as the radial distance of the SV from the PV increases. SVs are required to have $L_d^{xy}{>}1.6$ cm. We expect signal events to preferentially produce SVs with a large number of attached tracks, therefore we require SVs with track multiplicity of at least four. Interactions of primary collision particles (π, protons, etc.) with detector material, such as silicon sensors, cables, etc., are the major source of background. In order to quantify the material regions, we construct a map of SV density in data, using SV with track multiplicity of three, in the xy (see Fig. 1) and rz projections. SVs that occur in regions of high SV density are then removed. After this "pre-selection" is performed, the multijet background MC sample is normalized to the data (see Table I). Finally, at least two SVs are required in each event, and they are required to have $\Delta\mathcal{R}(SV1, SV2){>}0.5$, to prevent cases where a single true vertex is mis-reconstructed as two nearby separate vertices. No events in data have more than two SVs.

Two more variables are used to select the signal: SV invariant mass and SV collinearity. The invariant mass is reconstructed from the four-momenta of the outgoing tracks attached to a SV, assuming the pion mass for all particles. Collinearity is defined as the cosine of the angle between the vector sum of the momenta of the attached tracks and the direction to the SV from the PV. Depending on the signal point, one of these two variables is used to perform the final separation of signal and background. The quality of the background model is of primary importance so we develop a method of tuning the multijet

TABLE I: Summary of event selections, showing the remaining background, data, and signal events (for M_H=120 GeV and L_d=5 cm) after each selection. Background is normalized to data after pre-selection.

	$N_{\rm bkgd}$	$N_{\rm data}$	m_{HV}= 15 GeV	m_{HV}= 40 GeV
Produced	-	-	2712	2712
Initial selection	-	$4.9{\times}10^7$	235	173
Trigger	-	$4.9{\times}10^7$	174	77
SV $L_d^{xy}{>}1.6$ cm	-	$3.2{\times}10^7$	153	66
SV mult. $\geq$4	-	$1.8{\times}10^5$	72	25
SV density	$6.0{\times}10^4$	$6.0{\times}10^4$	60	15
Num. SV $\geq$2	37.5	26	5.1	0.6

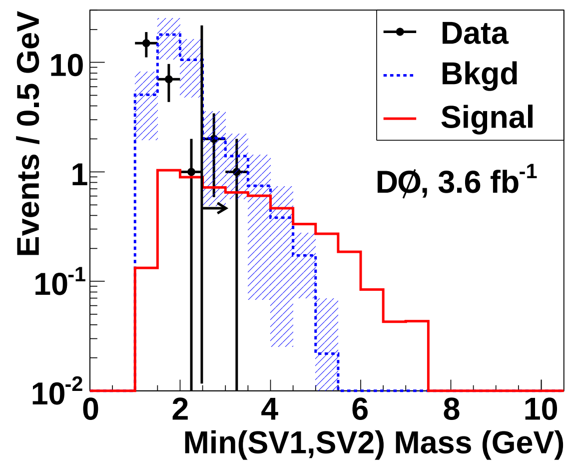

FIG. 2: The minimum mass of the two SVs, for data, background MC, and signal MC with M_H=120 GeV, m_{HV}=15 GeV, and L_d=5 cm. The hatched region shows the uncertainty on the background MC.

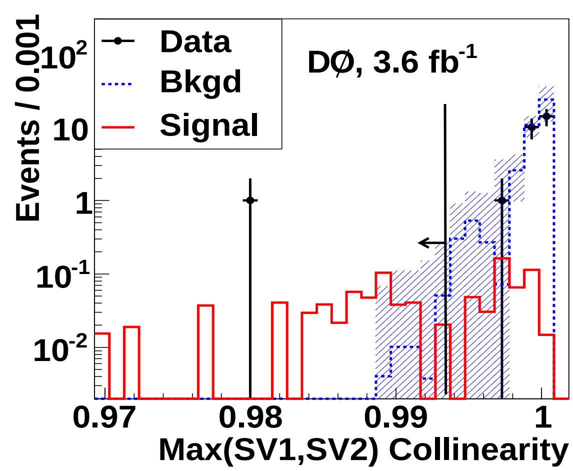

FIG. 3: The maximum collinearity of the two SVs, for data, background MC, and signal MC with M_H=120 GeV, m_{HV}=40 GeV, and L_d=5 cm. The hatched region shows the uncertainty on the background MC.

background simulation of the SV invariant mass and SV collinearity distributions to data. The events after preselection are divided into two distinct sets: the first contains events with only one SV (1SV), whereas the second contains events with at least two SVs (2SV). Since the signal content of the 2SV set is expected at about 4% as compared to only 0.04% for the 1SV set, we use the 1SV set to compare the data and MC and perform corrections to the MC. Gaussian smearing functions are applied to the background MC for the SV invariant mass and SV collinearity distributions, which are then also applied to all MC signal samples. For $m_{HV} < 20$ GeV, a requirement on the minimum SV mass in an event >2.5 GeV is most effective (Fig. 2). For heavier v-hadrons, we take advantage of the SV's decay products being more widely spread in angle, which is better measured than the invariant mass. Requiring the maximum SV collinearity in an event to be <0.9937 maximizes the expected significance (Fig. 3).

The uncertainty on the signal acceptance is dominated by the modeling of trigger efficiency and is (13–17)%. The uncertainty on the background due to the difference in track reconstruction efficiency between MC and data is estimated by using two methods of normalization and found to be 28%. We estimate the effect of smearing the MC samples by performing the entire analysis without smearing. For the requirements applied to the collinearity, smearing results in a difference of 18% on the multijet background yield and a negligible difference on the signal acceptance. Smearing also has no effect on the optimized requirement values. To estimate the uncertainty from requiring a small SV density, we compare the difference in the number of remaining events between multijet background and data before and after making the density requirement, and find agreement within (8–15)%. The uncertainty on the integrated luminosity is 6.1% [9].

The final results after all selections are summarized in Table II. No significant excess is observed, so 95% C.L. limits are set on $\sigma(H+X)\times\mathrm{BR}(H\to HVHV)\times\mathrm{BR}^2(HV\to b\bar{b})$ using a modified frequentist method [11], which includes all systematic uncertainties on signal acceptance, background, and luminosity. Depending on the signal parameters, Higgs boson production about 1–10 times the SM cross section is excluded, if the Higgs boson always decays to a pair of long-lived v-hadrons decaying only to $b\bar{b}$ (see Fig. 4). These results also provide the first constraints on pair-produced NLLPs decaying to b jets in the radial range of 1.6–20 cm at a hadron collider.

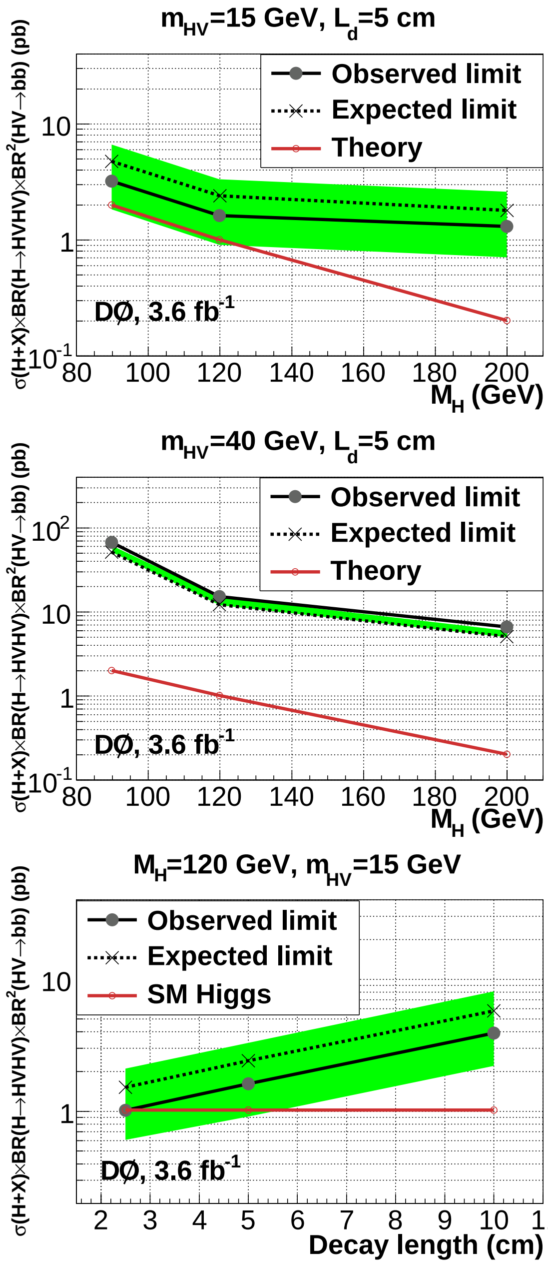

FIG. 4: The expected and observed 95% C.L. limits on $\sigma(H+X)\times\mathrm{BR}(H\to HVHV)\times\mathrm{BR}^2(HV\to b\bar{b})$ for each M_H studied, $m_{HV} = 15$, 40 GeV, and various values of v-hadron L_d. The green band shows the ±1 standard deviation on the expected limit. The reference Higgs boson cross section from the SM [10] is shown by the solid red line, which assumes 100% for $\mathrm{BR}(H\to HVHV)$ and $\mathrm{BR}(HV\to b\bar{b})$. (color online)

We thank the staffs at Fermilab and collaborating institutions, and acknowledge support from the DOE and NSF (USA); CEA and CNRS/IN2P3 (France); FASI, Rosatom and RFBR (Russia); CNPq, FAPERJ, FAPESP and FUNDUNESP (Brazil); DAE and DST (India); Colciencias (Colombia); CONACyT (Mexico); KRF and KOSEF (Korea); CONICET and UBACyT (Argentina); FOM (The Netherlands); STFC and the Royal Society (United Kingdom); MSMT and GACR (Czech Republic); CRC Program, CFI, NSERC and WestGrid Project (Canada); BMBF and DFG (Germany); SFI (Ireland); The Swedish Research Council (Sweden); CAS and CNSF (China); and the Alexander von Humboldt Foundation (Germany).

TABLE II: Results for each simulated signal: the numbers of background, signal, and data events after all selections, overall signal efficiency, SM Higgs production rate, and observed and expected 95% C.L. upper limits on the signal cross section.

M_H	m_{HV}	L_d	$N_{\rm bkgd} \pm {\rm stat} \pm {\rm sys}$	$N_{\rm sig} \pm {\rm stat} \pm {\rm sys}$	$N_{\rm data}$	Efficiency	SM Higgs (pb)	Limit obs. [exp.] (pb)
90 GeV	15 GeV	5 cm	$4.8 \pm 1.0 \pm 1.7$	$3.3 \pm 0.3 \pm 0.5$	3	0.06%	2.0	3.2 [4.7]
120 GeV	15 GeV	5 cm	$4.8 \pm 1.0 \pm 1.7$	$3.6 \pm 0.3 \pm 0.5$	3	0.13%	1.1	1.6 [2.4]
120 GeV	15 GeV	2.5 cm	$4.8 \pm 1.0 \pm 1.7$	$5.7 \pm 0.3 \pm 0.7$	3	0.21%	1.1	1.0 [1.5]
120 GeV	15 GeV	10 cm	$4.8 \pm 1.0 \pm 1.7$	$1.5 \pm 0.2 \pm 0.3$	3	0.06%	1.1	3.9 [5.7]
200 GeV	15 GeV	5 cm	$4.8 \pm 1.0 \pm 1.7$	$0.8 \pm 0.1 \pm 0.1$	3	0.16%	0.2	1.3 [1.8]
90 GeV	40 GeV	5 cm	$0.07 \pm 0.07 \pm 0.02$	$0.15 \pm 0.07 \pm 0.03$	1	0.003%	2.0	67 [51]
120 GeV	40 GeV	5 cm	$0.07 \pm 0.07 \pm 0.02$	$0.38 \pm 0.07 \pm 0.06$	1	0.01%	1.1	16 [12]
200 GeV	40 GeV	5 cm	$0.07 \pm 0.07 \pm 0.02$	$0.16 \pm 0.03 \pm 0.02$	1	0.03%	0.2	6.5 [5.1]

[a] Visitor from Augustana College, Sioux Falls, SD, USA.
[b] Visitor from Rutgers University, Piscataway, NJ, USA.
[c] Visitor from The University of Liverpool, Liverpool, UK.
[d] Visitor from Centro de Investigacion en Computacion - IPN, Mexico City, Mexico.
[e] Visitor from ECFM, Universidad Autonoma de Sinaloa, Culiacán, Mexico.
[f] Visitor from Helsinki Institute of Physics, Helsinki, Finland.
[g] Visitor from Universität Bern, Bern, Switzerland.
[h] Visitor from Universität Zürich, Zürich, Switzerland.
[‡] Deceased.

[1] M. J. Strassler and K. M. Zurek, Phys. Lett. B **651**, 374 (2007).
[2] M. J. Strassler and K. M. Zurek, Phys. Lett. B **661**, 263 (2008).
[3] R. Barate *et al.*, Phys. Lett. B **565**, 61 (2003).
[4] S. Chang, R. Dermisek, J. F. Gunion, and N. Weiner, Ann. Rev. Nucl. Part. Sci. **58**, 75 (2008).
[5] D0 Collaboration, V. Abazov *et al.*, Nucl. Instrum. Methods Phys. Res. A. **565**, 463 (2006).
[6] T. Sjöstrand *et al.*, Comput. Phys. Commun. **135**, 238 (2001).
[7] R. Brun and F. Carminati, CERN Program Library Long Writeup W5013, 1993 (unpublished).
[8] G. C. Blazey *et al.*, arXiv:hep-ex/0005012 (2000).
[9] T. Andeen *et al.*, FERMILAB-TM-2365 (2007).
[10] D. de Florian and M. Grazzini, Phys. Lett. B **674**, 291 (2009).
[11] T. Junk, Nucl. Instrum. Methods A. **434**, 435 (1999).